A Journal of the Gesellschaft Deutscher Chemiker

Angewandte International Edition GDCh Chemie

www.angewandte.org

Accepted Article

Title: Plasma-Enabled Process with Single-Atom Catalysts for Sustainable Plastic Waste Transformation

Authors: Xiao Yu, Zhiqiang Rao, Guoxing Chen, Yuantao Yang, Songhak Yoon, Lina Liu, Zeai Huang, Marc Widenmeyer, Heng Guo, Gert Homm, Ulrike Kunz, Xingmin Liu, Emanuel Ionescu, Leopoldo Molina-Luna, Xin Tu, Ying Zhou, and Anke Weidenkaff

To be cited as: *Angew. Chem. Int. Ed.* **2024**, e202404196

Link to VoR: https://doi.org/10.1002/anie.202404196

WILEY VCH

10.1002/anie.202404196

Plasma-Enabled Process with Single-Atom Catalysts for Sustainable Plastic Waste Transformation

Xiao Yu[1#], Zhiqiang Rao[2#], Guoxing Chen[1*], Yuantao Yang[2], Songhak Yoon[1], Lina Liu[3], Zeai Huang[2*], Marc Widenmeyer[4], Heng Guo[2], Gert Homm[1], Ulrike Kunz[3], Xingmin Liu[4], Emanuel Ionescu[1,4], Leopoldo Molina-Luna[4], Xin Tu[5], Ying Zhou[2*], Anke Weidenkaff[1,4]

[1]Fraunhofer Research Institution for Materials Recycling and Resource Strategies IWKS, Brentanostraße 2a, 63755 Alzenau, Germany

[2] New Energy and Materials, Southwest Petroleum University, Chengdu 610500, China

[3]College of Environmental Science and Engineering, Ministry of Education Key Laboratory of Pollution Processes and Environmental Criteria, Nankai University, Tianjin, 300350, China

[4]Department of Materials and Earth Sciences, Technical University of Darmstadt, Peter-Grünberg-Str. 2, 64287 Darmstadt, Germany

[5]Department of Electrical Engineering and Electronics, University of Liverpool, Liverpool L69 3GJ, United Kingdom

Abstract

The escalating issue of plastic waste generation has prompted the search for an effective solution to address these challenges. In this study, we present a novel plasma-enabled strategy for the rapid breakdown of various types of plastic wastes, including mixtures, into high-value carbon nanomaterials and hydrogen. The H_2 yield and selectivity achieved through the implemented catalyst-free plasma-enabled strategy are 14.2 and 5.9 times higher, respectively, compared to those obtained with conventional thermal pyrolysis under similar conditions. It is noteworthy that this catalyst-free plasma alone approach yields a significantly higher energy yield of H_2 (g_{H2}/kWh) compared to other pyrolysis processes. By coupling plasma pyrolysis with thermal catalytic process, employing of 1 wt.% *M*/CeO_2 (*M* = Fe, Co, and Ni) atomically dispersed catalysts can further enhance hydrogen production. Specifically, the 1 wt.% Co/CeO_2 catalyst demonstrated excellent catalytic performance throughout the 10 cycles of plastic waste decomposition, achieving the highest H_2 yield of 46.7 mmol/$g_{plastic}$ (equivalent to 64.4% of theoretical H_2 production) and nearly 100% hydrogen atom recovery efficiency at the 7^{th} cycle. Notably, the H_2 yield achieved over the atomically dispersed Fe on CeO_2 surface (1 wt.% Fe/CeO_2) in the integrated plasma-thermal catalytic process is comparable to that obtained with Fe particles on CeO_2 surface (10 wt.% Fe/CeO_2). This outcome, demonstrated with single-atom

catalysts, offers a promising avenue for cost-effective and efficient chemical plastic recycling. Through a combination of experimental and computational efforts, we have provided an in-depth understanding of the catalytic mechanisms of the investigated single atom catalysts in the developed plasma-enabled process. This innovative and straightforward approach provides a promising and expedient strategy for continuously converting diverse plastic waste streams, including mixed and contaminated sources, into high-value products conducive to a circular plastic economy.

Email: guoxing.chen@iwks.fraunhofer.de; zeai.huang@swpu.edu.cn;
yzhou@swpu.edu.cn

Keywords: plasma pyrolysis, single atom catalyst, plastic waste, H_2, carbon nanotube

Introduction

Plastic, as an incredibly versatile material, has found widespread applications in various aspects of life due to its lightweight, durability, chemical resistance, design flexibility, and affordability. The substantial demand for plastics in daily life has led to a consistent and exponential increase in global production over the past few decades. In 2022, approximately 400 million metric tons (Mt) of plastic were produced worldwide [1]. Predictions indicate that the demand for plastic is poised to continue expanding, potentially exceeding 500 Mt by 2050[2]. Concomitant with the burgeoning production of plastic, the generation of post-consumer waste has expanded in tandem. A substantial proportion of plastic products were designed for single-use, enhancing further the issue of plastic waste formation. In year 2019, 353 Mt plastic waste were formed, however mostly found its way into landfills or the natural environment. Only 9% of the plastic waste underwent recycling[3,4]. Notably, this recycling rate exhibited significant variation depending on the geographical region and the type of plastic[5]. The recycling of multi-type plastic mixtures is especially difficult and challengeable. In 2020, Europe only managed to recycle 5% of its mixed plastic waste[6]. Further development of robust and effective methods for processing such plastic waste mixtures is essential.

Conventional plastic recycling methods include energy recovery and mechanical recycling. Energy recovery, also referred to as incineration, can recover some of the energy within plastics. However, it is environmentally unfriendly due to the generation of toxic gases or materials and large amounts of carbon dioxide emissions favoring the climate change. Mechanical recycling is energy- and cost effective, but shows its drawbacks in the preceding process such as separation of plastic mixtures and elimination of attached residues. In addition, the reprocessed

plastic displays reduced levels of both durability and flexibility[7]. Comparing to traditional recycling mechanism, chemical recycling is considered as an alternative method for upcycling plastic wastes [8], especially for mixed typed plastics or multilayer plastics. It can directly convert the waste into chemical products such as liquid fuels[9], carbonaceous materials[10], syngas[11] and H_2-rich gases [12] via gasification or pyrolysis. Simultaneous production of H_2 and carbon nanomaterials via catalytic pyrolysis of plastic wastes has attracted the attention of many researchers in the recent years. The two-stage catalytic thermal process (as shown in Figure S1(a)) have been developed by many groups for the co-production of H_2 and carbon nanotubes[13–15]. Wasted plastics are decomposed into hydrocarbon gases at the first stage, which then pass a second stage and further reformed into H_2-rich gases and carbonaceous materials via a catalytic process with or without the introduction of water vapor[16]. Nevertheless, this method can only achieve an acceptable product yield with a long reaction period at high temperatures, demanding substantial energy consumption and resulting in a low energy yield of H_2 (g_{H2}/kWh). Several studies found that integrating a non-thermal plasma reactor to proceed the second stage (as shown in Figure S1(b)) can significantly decrease the reaction temperature from around 800 °C to below 250 °C[17,18], thereby reducing the heating energy. Although employing a dielectric barrier discharge, this two-stage low-temperature plasma catalytic process still shares the same mechanism with the traditional two-stage thermal pyrolysis. The energy needed for both plastic degradation and catalyst activation are supplied by furnaces. Similar to the pure thermal two-stage pyrolysis, the two-stage low-temperature plasma process can only achieve less competitive H_2 yield and calls for a long reaction time. Microwave-initiated catalytic pyrolysis (as shown in Figure S1(c)) has recently been found as a promising method for upcycling wasted plastics, which not only can reach reasonable product yields within short time[4,19,20] but also achieve a high energy yield of H_2 (g_{H2}/kWh). However, as plastics cannot directly react with microwaves, the utilization of suitable metal catalysts as heat susceptors to uniformly mix with plastics and deliver energy is essential for this method. Several studies showed the ratio of catalysts to plastics plays a crucial role in this process. A ratio of at least 1:1 or higher is required to attain satisfactory yields[21–23]. Besides, how to solve the gradual catalyst deactivation, caused by the accumulation of generated solid carbonaceous on the catalysts' surface, remains a challenge. Both mentioned points necessitate increased investment and thus reduce the economic efficiency of microwave-initiated decomposition process of plastics, especially when considering its scalability to industrial applications.

An approach with upscaling possibility for effectively recycling of plastic wastes is extremely needed to be developed. A combination of different pyrolysis methods, which can

take their individual advantages, could be a solution to achieve valuable outcomes with high level energy and economic efficiency. Furthermore, the selection of catalysts has a significant impact on the catalytic pyrolysis process. Transition metal-based catalysts, extensively applied in thermal as well as microwave-initiated decomposition process, are promising options. However, traditional metal catalysts can only present a medium atomic efficiency because the functional metal particles usually exist as nanoparticle clusters. Furthermore, high prices of many transition metals, are rising economic concerns. Single-atom catalysts (SACs), are regarded as a promising choice to maximize the atomic efficiency of the metal-based catalysts due to the atomic dispersion of functional metal atoms. Its excellent catalytic performance shown in hydrogen production[24], may further enhance the yields of plastic wastes pyrolysis. Moreover, the deactivated catalysts due to the on-surface accumulating produced carbon nanomaterials, together with the solid products could be directly reused in electrochemical applications for chemical production [25], further increasing the economic performance of the entire proposed upcycling strategy.

Herein, we demonstrate an innovative plasma-enabled strategy for rapid deconstruction of various types of plastic wastes as well as their mixtures into high value-added products. The catalyst-free plasma alone process (as shown in Figure S2) can degrade various plastic wastes or their mixtures within several minutes after switching on the plasma generator. For example, in the case of using discarded milk containers (HDPE), a substantial H_2 yield of 43.3 mmol/$g_{plastic}$ (equivalent to 48.7% of the theoretical H_2 production) with a corresponding H_2 selectivity of 60.6% makes it easily distinguished from conventional thermal pyrolysis by the outstanding production efficiency. In our developed plasma-enabled process, the plastic decomposition is primarily induced by plasma itself. Different from the microwave-initiated catalytic process, our approach obviates the necessity for absorptive materials and catalysts. Employing catalyst-free plasma alone process can prove highly effective in efficiently decomposing plastic waste into hydrogen and valuable carbon materials. To enhance the quality of the carbon materials produced and to advance the control and selectivity of product yield, the plasma alone pyrolysis process was integrated with a subsequent thermal catalytic process (see Figure S3). In this combined plasma-thermal catalytic pyrolysis process, 1 wt.% *M*/CeO2 (M = Fe, Co, and Ni) single-atom catalysts were utilized. All the three investigated SACs were observed to function effectively for up to 5 cycles. Co/CeO_2 exhibited the best activity among the studied catalysts, succeeded 10 effective cycles of plastic waste decomposition, achieving the highest H_2 yield of 46.7 mmol/$g_{plastic}$ (equivalent to 64.4% of theoretical H_2 production) at the 7^{th} cycle. A combination of density functional theory (DFT) calculations and experimental

measurements was employed to deepen the understanding of the catalytic mechanisms of the investigated single atom catalysts during the integrated thermal process in the developed plasma-thermal catalytic pyrolysis process. Our findings may open a new avenue for effectively upcycling plastic waste with a high upscaling possibility and low energy and economic investment.

Results and Discussion

Plasma pyrolysis approach for deconstruction of different types of plastic waste and their mixtures

In this study, the plasma-enabled approach (both catalyst-free plasma alone and coupling with thermal catalytic process) for decomposing the various types of plastics collected from our daily life (fruit packing boxes (PP), milk containers (HDPE), packing bags (LDPE), yoghurt containers (PS), drink bottles (PET) and their mixtures) was investigated for co-producing H_2 and carbon materials towards both sustainable hydrogen economy and carbon economy (See Figure 1(a)). To introduce our innovative plasma-assisted plastic waste upcycling method, we start with the catalyst-free plasma alone pyrolysis process (as shown in Figure S2) to establish it as a comparable reference. Comprehensive details about the developed system and the reactors are included in the supporting information (See Figure S2-S5).

Figure 1 indicates the results of decomposition of these mentioned five most common daily-life plastic wastes and their mixtures in the plasma pyrolysis process. Every single experiment has been repeated for three times to avoid systematic or experimental errors. The average value was applied for analysis and the statistically results were concluded into the diagram as error bars. The theoretical H_2 yield describes the highest H_2 yield, when the studied plastic is fully converted into hydrogen and carbonaceous materials. For PP, HDPE, LDPE and their mixture, the theoretical H_2 yield is about 71.4 mmol/$g_{plastic}$. For PS and PET, the theoretical H_2 yield are 38.4 mmol/$g_{plastic}$ and 20.8 mmol/$g_{plastic}$, respectively. In comparison to conversional thermal pyrolysis under similar conditions, experiments using the plasma pyrolysis process (see Table S1) for decomposition of discarded milk containers (HDPE) result in a significantly higher H_2 yield and selectivity, which are enhanced by 14.2 and 5.9 times higher, respectively. Simultaneously, negligible liquid yields can be observed in plasma pyrolysis cross various types of plastics (see Figure 1(b) and Table S1-S2). Based on the study by X. Jie et al. [20], where the mass balance is defined as the sum of gas and solid yields where limited liquid products are formed, we adopted the same calculation method. The results, summarized in Table S1-S2, show a mass balance close to 100% in most of the cases studied. These results clearly indicate

that the plasma route can significantly reduce side reactions and hence produces outstandingly high H_2 yields. As depicted in Figure 1(c), utilizing the investigated PP (vegetable packing boxes), HDPE (milk containers) and LDPE (sample bags) plastic waste in the developed plasma pyrolysis process delivers similar H_2 yields of around 30 mmol/$g_{plastic}$ (equivalent to ~42% of the theoretical H_2 yield). The slight differences could be attributed to the additives contained in the employed real-world plastic waste (See Figure S6). As illustrated in Figure 1(c) and (d), the plasma method proves to be efficient across different plastic types. In particular, the H_2 yield from drink bottles (PET) conversion reached 14.0 mmol/$g_{plastic}$ (~ 67.5% of the theoretical H_2 yield), accompanied by a corresponding H_2 selectivity of 77.3% during the plasma pyrolysis process. It is worth emphasizing that the catalyst-free plasma alone method also demonstrates effectiveness in decomposing mixed plastic wastes. When processing a combination of five distinct types of plastic waste materials (20 wt.% drink bottles (PET), 20 wt.% milk containers (HDPE), 20 wt.% fruit packing boxes (PP), 20 wt.% packing bags (LDPE), and 20 wt.% yoghurt containers (PS)), the H_2 yield can reach 26.2 mmol/$g_{plastic}$ (equivalent to ~47.8% of the theoretical H_2 yield) with a corresponding H_2 selectivity of about 63.2%. It is important to highlight that in the plasma alone process across all examined cases, C_2H_2 overwhelmingly surpasses all other gas products, excluding H_2, as depicted in Figure 1(d). This observation stands in strong contrast to findings reported in the literature for thermal pyrolysis and microwave-initiated procedures [4,26]. As shown in Figure 1 (d), H_2 and C_2H_2 take over 80% of the gaseous product composition in all studied cases, which is significantly different from our previous study of thermal pyrolysis[27], where CH_4 always had the largest portion in the gaseous product. By contrast, the composition of CH_4 in the gas evolved from plasma alone process is under 9% across all examined cases, and it varied along with the change of plastic types as well as mixture composition. The production of C_2H_6 was quite limited no matter which plastic was utilized as the feedstock in the plasma pyrolysis process. This limitation arises from the reactive nature of plasma. Excited species and highly energetic electrons provided by the plasma can effectively break chemical bonds within plastics, causing longer C_xH_y molecules to break up into smaller ones, which is the main difference between plasma pyrolysis and thermal pyrolysis. The results demonstrated that the designed plasma-enabled process can be a promising way for mixed plastic waste upcycling. It is noteworthy to emphasize that, within the plasma-only process, valuable carbon materials of high quality can be directly generated from diverse types of plastic waste (see Figure S7). The morphology of the produced carbon materials is not significantly influenced by the specific types of plastic employed.

10.1002/anie.202404196

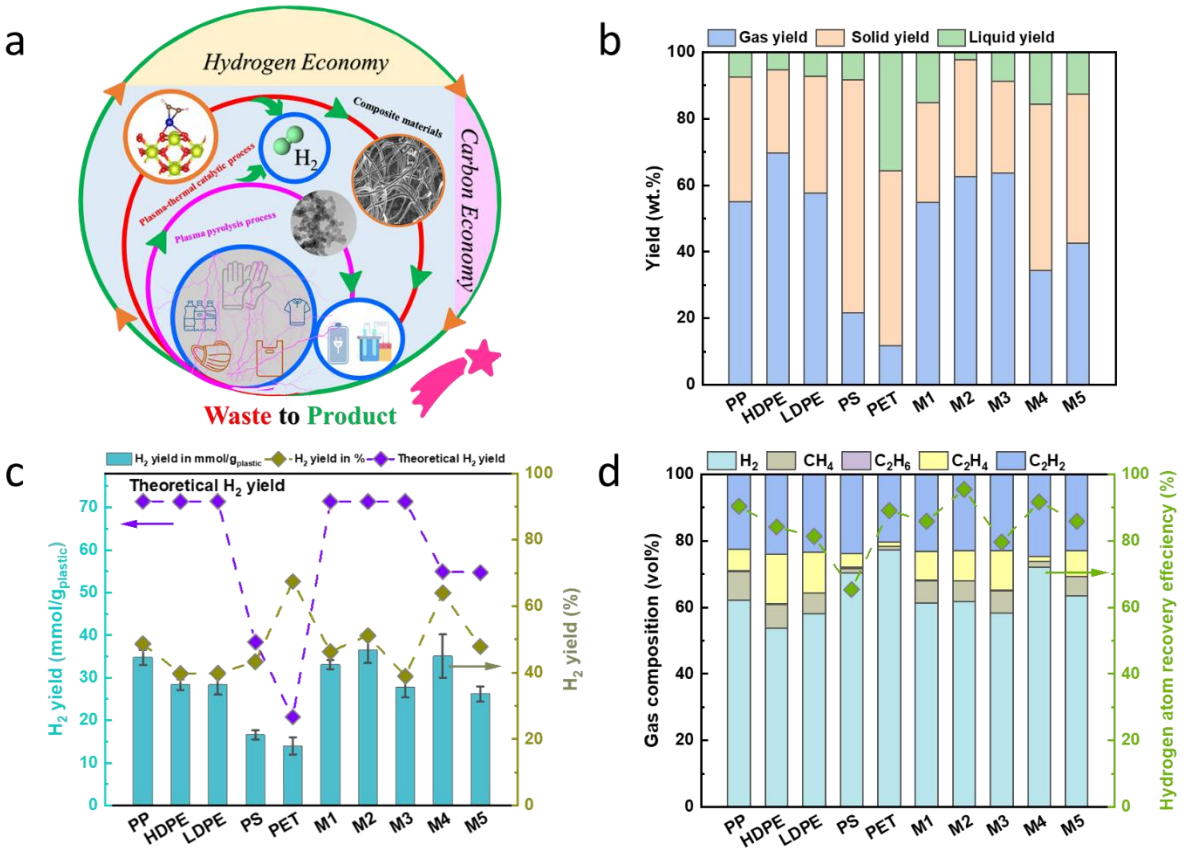

Figure 1. (a) Schematic of the proposed "waste to product" concept for sustainable plastic waste upcycling. Plasma pyrolysis of different types of real-world plastic wastes and their mixtures: (b) yields of gas, solid and liquid (wt.%), (c) H_2 yield (mmol/$g_{plastic}$ and %) and theoretical H_2 yield (mmol/$g_{plastic}$), (d) gas composition (vol%) and hydrogen atom recovery efficiency (%).0.4 g of plastic is used for all the tests. The mixture of different types of plastic studied in the Figure 1 is defined as follows: M1, M2 and M3 are the mixtures of PP, LDPE and HDPE with weight ratios of 2:1:1, 1:2:1 and 1:1:2, respectively; M4 is the mixture of LDPE, HDPE and PS with a weight ratio of 1:1:2; M5 is the mixture of all five types of studied plastics with a weight ratio of 1:1:1:1:1.

Plasma-thermal catalytic pyrolysis of plastic waste over *M*/CeO_2 (*M* = Ni, Co, and Fe) single atom catalysts

In order to further improve the performances for co-producing H_2 and high value-added carbon products from plastic wastes, catalysts are essential to be introduced into the plasma pyrolysis process. A thermal catalytic process is coupled with the output line of the discussed plasma alone process (as shown in Figure S3). Examining single atom catalysts as potential catalysts offers a promising choice to maximize the atomic efficiency of the metal-based catalysts, which will reduce the cost of the catalyst significantly. Thus, three SACs of 1 wt.% *M*/CeO_2 (*M* = Fe, Co, and Ni) were prepared and evaluated regarding their catalytic

10.1002/anie.202404196

performance in the plasma-thermal catalytic pyrolysis of wasted milk containers (HDPE). Figure 2(a) shows the X-ray diffraction (XRD) patterns of the fresh supported single-atom catalysts and pure CeO_2 support. All XRD reflections of the studied samples can be assigned to the characteristic reflections of CeO_2 fluorite phase, which is in a good agreement with the Raman results as shown in Figure S8. Similar to the Raman spectra of pure CeO_2 support, a strong band at about 467 cm^{-1} in the Raman spectra for the different single-atom catalysts, which can be linked to the vibrational mode (F2g) of the cubic fluorite structure. The CeO_2 nanorods were chosen as the catalyst support due to its surface defects that can be used to anchor metal atoms. The detailed structural information was obtained by Rietveld refinements of XRD patterns of the fresh catalysts. As observed in Figure 2(b) and Figure S9, all collected diffraction data are best fitted by a cubic phase. The high-resolution high-angle annular dark-field scanning transmission electron microscopy (HR-HAADF-STEM) images of fresh 1 wt.% *M*/CeO_2 (*M* = Fe, Co, and Ni) were presented in Figure 2(c), indicating that the surface of cerium oxide nanorods is free from visible metal particles. No distinct bright spots can be observed due to the higher atomic content of Ce than that of the deposited metal *M* (*M* = Fe, Co, or Ni). The corresponding energy dispersive spectrometry (EDS) elemental distribution mapping shown in Figure 2(d) and Figure S10 further confirms the highly dispersed state of the deposited metals.

10.1002/anie.202404196

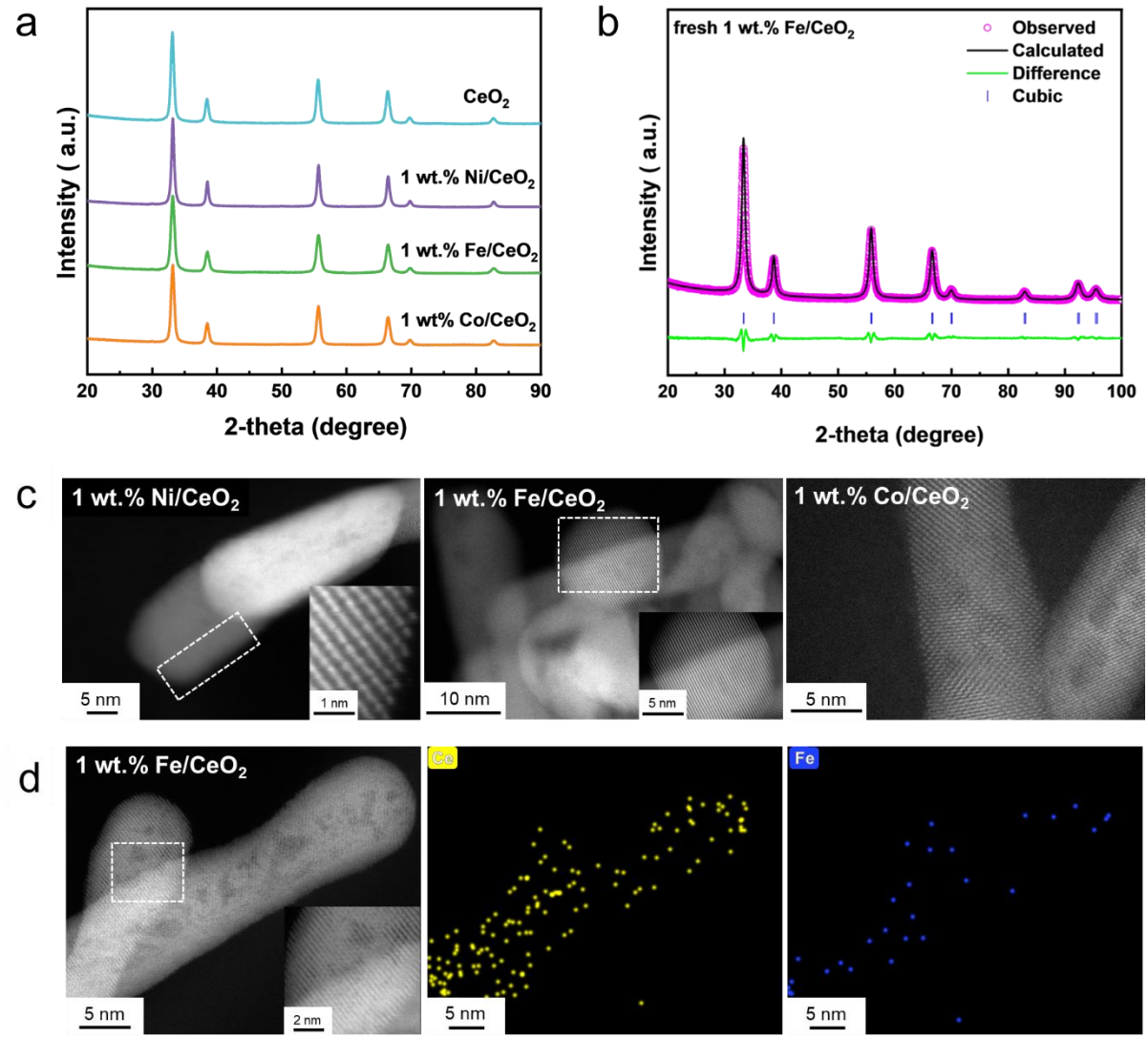

Figure 2. Characterization on the fresh single-atom catalysts. (a) XRD patterns of the fresh single atom catalysts *M*/CeO_2 (*M* = Fe, Co, and Ni) and pure CeO_2 support. (b) Rietveld refinement of the XRD pattern of fresh 1 wt.% Fe/CeO_2 catalyst. (c) HR-HAADF-STEM images of fresh single atom catalysts *M*/CeO_2 (*M* = Fe, Co, and Ni). (d) EDS elemental mapping images of fresh 1 wt.% Fe/CeO_2 catalyst.

Figure 3 depicts the H_2 production performance employing single-atom catalysts based on 1 wt.% *M*/CeO_2 (*M* = Ni, Co, Fe) in the plasma-thermal catalytic pyrolysis of discarded milk containers (HDPE). The integration of a thermal catalytic process employing the studied single atom catalysts into the plasma enabled decomposition process results in a significant increase in both H_2 yield and selectivity compared to both the catalyst-free plasma alone process and the plasma-thermal process over CeO_2 support. 1 wt.% Co/CeO_2 presented the best catalytic performance with a H_2 yield of 41.7 mmol/$g_{plastic}$, following by 1 wt.% Ni/CeO_2, and 1 wt.% Fe/CeO_2 with 38.3 mmol/$g_{plastic}$ and 37.8 mmol/$g_{plastic}$, respectively. It is particularly noteworthy

10.1002/anie.202404196

that the H_2 yield attained with the 1 wt.% Fe/CeO_2 single-atom catalyst is comparable to that achieved with the 10 wt.% Fe/CeO_2 nanoparticle catalyst (38.5 mmol/$g_{plastic}$). This result, showcased with single-atom catalysts, opens up a promising path for plastic recycling which can be both cost-effective and efficient.

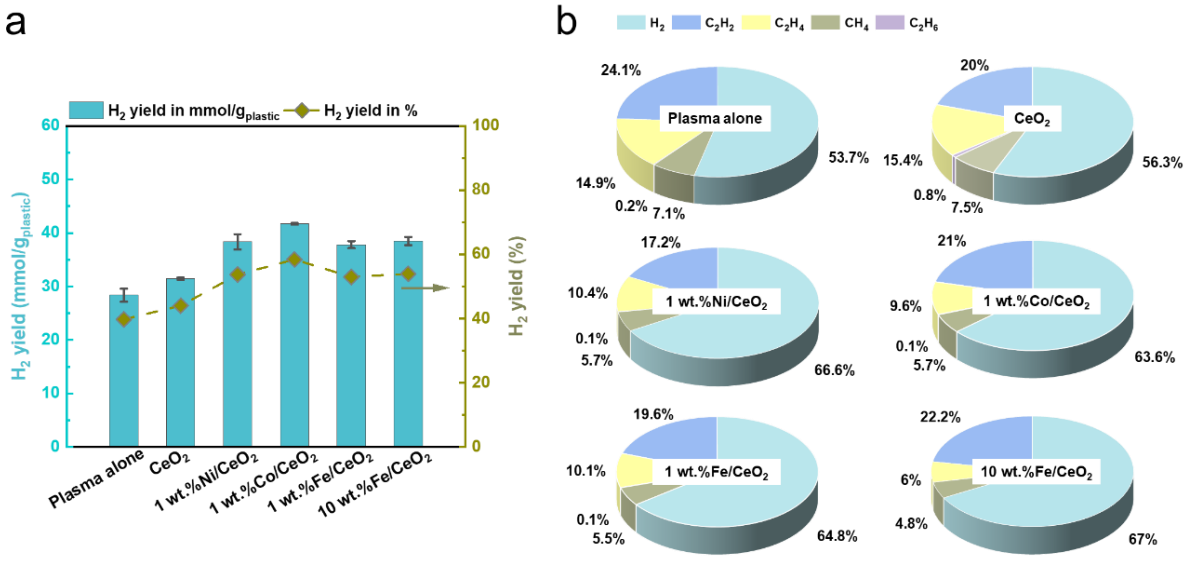

Figure 3. (a) H_2 yield (mmol/$g_{plastic}$) and (b) gas composition (vol%) in the catalyst-free plasma alone process and plasma-thermal catalytic process of decomposing the discarded milk containers (HDPE) over CeO_2 support, 1 wt.% *M*/CeO_2 (*M* = Ni, Co, Fe) single atom catalysts and 10 wt.% Fe/CeO_2 nanoparticle catalyst.

Successive cycles of plasma-thermal catalytic pyrolysis of discarded milk containers (HDPE) over *M*/CeO_2 single atom catalysts

Integrating the plasma process with a thermal catalytic process as a tandem technology not only enhances hydrogen production but also yields value-added carbon materials. Since the plastic and catalyst are separate in our developed plasma-thermal catalytic system, allowing for the consistent transformation of diverse types of plastic waste streams into valuable products, which also provide a promising way for avoiding catalyst deactivation. As shown in Figure 4 and Table S3-S5, sequential cycle measurements were conducted with the 1 wt.% *M*/CeO_2 (*M* = Ni, Co, Fe) single atom catalysts to assess their deactivation tendencies and sustained catalytic performance in the developed plasma-thermal catalytic pyrolysis process. Discarded milk containers made of HDPE served as the feedstock which was added consecutively without the

10.1002/anie.202404196

addition of fresh catalyst between each cycle. Each individual single atom catalyst underwent five successive cycles.

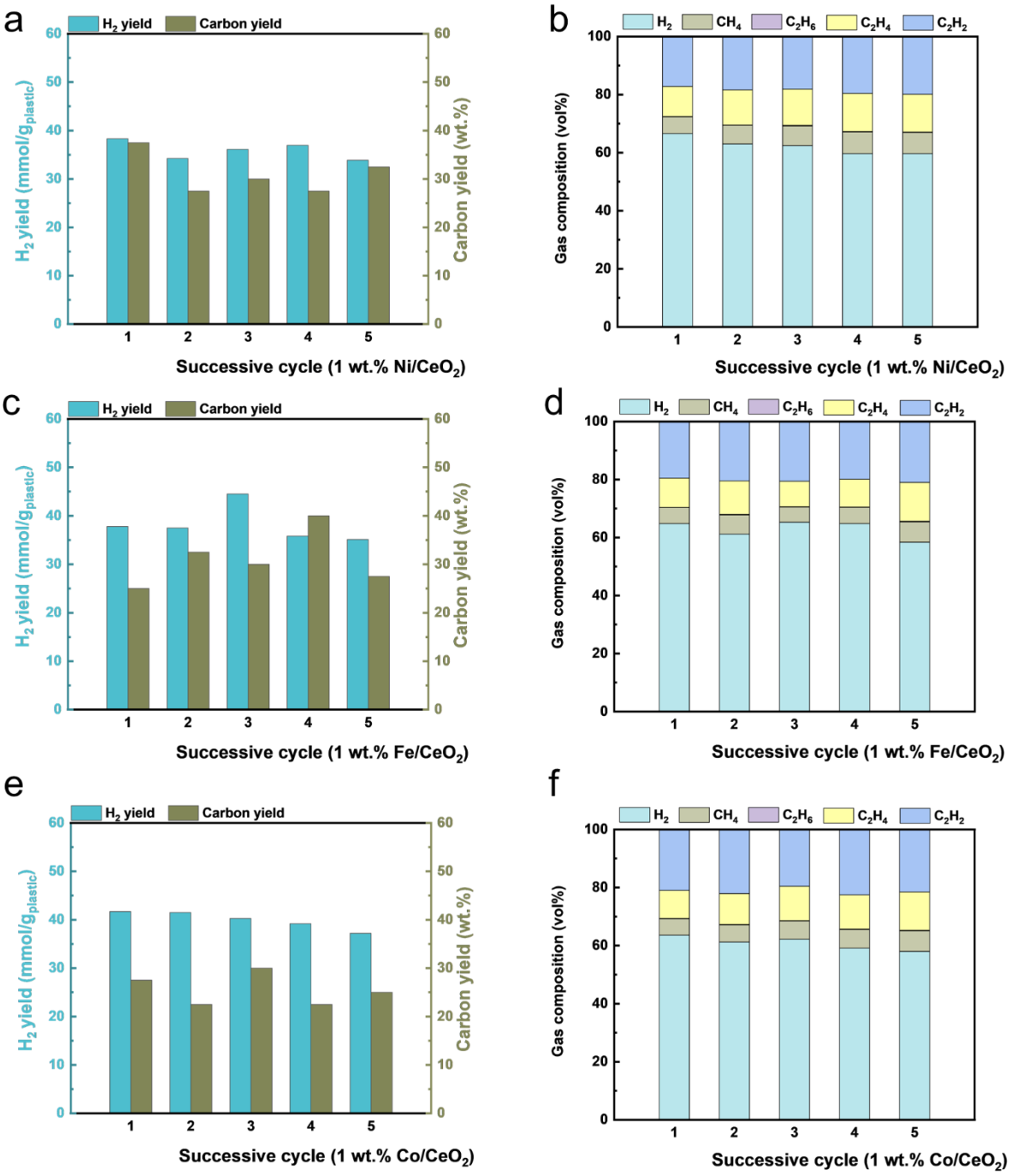

Figure 4. Successive cycles of the deconstruction of discarded milk containers (HDPE) in the plasma-thermal catalytic pyrolysis over 1 wt.% *M*/CeO_2 (*M* = Ni, Fe, Co) catalysts. (a, c, e) H_2 yield (mmol/$g_{plastic}$) and carbon yield (wt.%). (b, d, f) gas composition (vol%). 0.4 g of plastic is added into each cycle as feedstock, and the catalyst is 0.4 g throughout the entire cyclic measurement without further addition.

Generally, the H_2 yield exhibited a slight decrease but remained at a consistently high level throughout the entire cyclic testing. The Ni- and Co-based SACs achieved their maximum

10.1002/anie.202404196

yields in the initial cycle, yielding 38.3 mmol/$g_{plastic}$ and 41.7 mmol/$g_{plastic}$, respectively. Notably, 1 wt.% Fe/CeO_2 boosted its catalytic performance during the third cycle with a H_2 yield of 44.5 mmol/$g_{plastic}$. A substantial hydrogen yield of 37.2 mmol/$g_{plastic}$ was consistently maintained through five consecutive measurement cycles.

To investigate the stability of the *M*/CeO_2 single-atom catalysts in the plasma-thermal catalytic system, we characterized the spent catalysts (after 5 successive cycles) using XRD Rietveld refinements. Comparing the Rietveld refinements of the XRD patterns of fresh *M*/CeO_2 (shown in Figure 2(b) and Figure S9) with those of the spent catalysts (shown in Figure 5(a) and Figure S11) reveals that the catalysts maintain their original structure with almost no change. The limited differences in cell parameters between the fresh and spent catalysts, as shown in Table S6, further confirm the chemical stability of the studied catalysts in the plasma-thermal catalytic process. To further investigate the reusability of the spent catalysts, we examined Fe/CeO_2 as an example using HR-HAADF-TEM. The images and corresponding mapping shown in Figure 5(b) indicate that the Fe atoms remain well-dispersed after five cycles. To disclose the electronic structures and coordination states in the spent Fe/CeO_2 catalyst, we performed X-ray absorption spectroscopy (XAS) of the Fe K-edge. As shown in Figure 5(c), comparison with the referential edge position indicates that Fe is present in its oxidized state in the spent catalyst. A significant signal at around 1.6 Å in the Fourier-transformed k^2-weighted extended X-ray absorption fine structure (EXAFS) (Figure 5(d)) is observed, which corresponds to Fe-O coordination. In conclusion, the studied catalysts generally maintain their coordination and structure after five cycles, demonstrating their stability and reusability in the plasma-thermal catalytic process.

To further assess the stability of the *M*/CeO_2 single-atom catalysts in the plasma-thermal catalytic system, we conducted an additional five successive test cycles under the same conditions using the Co/CeO_2 catalyst, directly following the previous five-cycle measurements, as shown in Figure 4(e) and (f). As demonstrated in Figure 5(e), Figure 5(f), Figure S12, and Table S4, a high hydrogen yield of 42.9 mmol/$g_{plastic}$ was maintained even after 10 successive cycles, with the highest H_2 yield of 46.7 mmol/$g_{plastic}$ achieved in the 7th cycle. This demonstrates the excellent capability of transforming plastics into H_2 and high-value carbon products by coupling the plasma pyrolysis process with the thermal catalytic process. Simultaneously, a carbon yield ranging from 25 wt.% to 30 wt.% per cycle throughout the continuous five-cycle measurements resulted in a total production of approximately 0.55 g of carbon materials. The spent Co/CeO_2 catalyst after 10 successive cycles was also analyzed by Rietveld refinements of the XRD pattern, as shown in Figure S13(a). The XRD patterns of the

10.1002/anie.202404196

spent Co/CeO_2 catalyst after 10 successive cycles are similar to those after 5 successive cycles (see Figure S13(b)), and the Rietveld refinement results indicate that the catalysts remained stable in a cubic phase. This underscores the impressive reusability of the 1 wt.% Co/CeO_2 single-atom catalyst in the plasma-thermal catalytic pyrolysis process for converting real-world plastic waste into both H_2 and high-value carbon products.

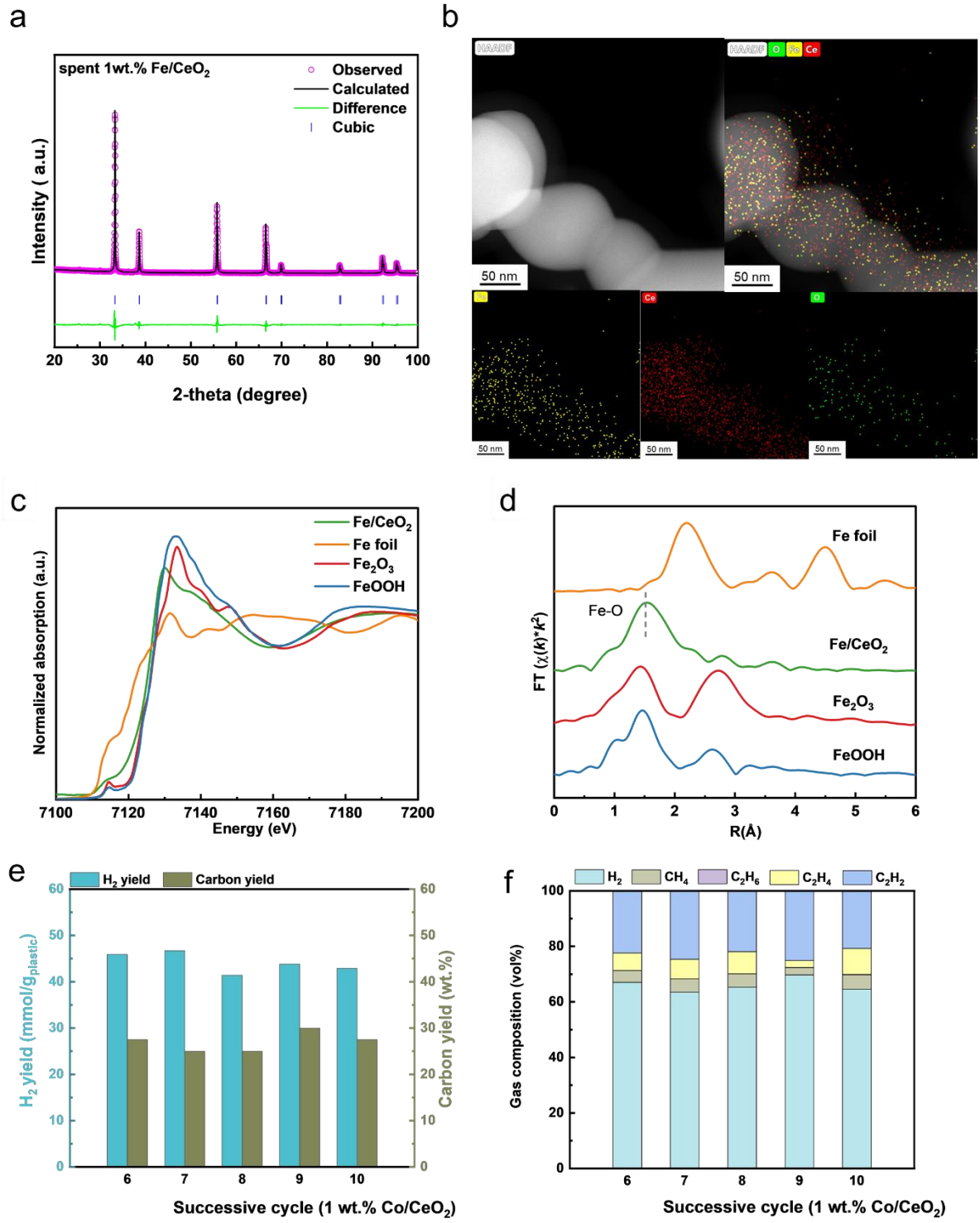

10.1002/anie.202404196

Figure 5. (a) Rietveld refinement of the XRD pattern of spent 1 wt.% Fe/CeO_2 catalyst after 5 cycles. (b) HR-HAADF-STEM images with EDS elemental mapping images of spent 1 wt.% Fe/CeO_2 catalyst after 5 cycles. (**c**) The Fe K-edge XANES spectra. (d) k^2-weighted Fourier transform EXAFS spectra of Fe_2O_3, Fe foil, FeOOH, and spent 1wt.% Fe/CeO_2 after 5 cycles. Additional 5 successive cycles of the deconstruction of discarded milk containers (HDPE) in the plasma-thermal catalytic process using the 1wt.% Co/CeO_2 catalyst. (e) H_2 yield ($mmol/g_{plastic}$) and carbon yield (wt.%). (f) gas composition (vol%). 0.4 g of plastic is added into each cycle as feedstock, and the catalyst is 0.4 g throughout the entire cyclic measurement without further addition.

Characterization of the produced carbonaceous materials from plasma-thermal catalytic pyrolysis approach

Figure 6(a) and Figure S14 display low- and high-magnification SEM images of the carbon nanomaterials generated over the examined three SACs during the successive cycles of plasma-thermal catalytic pyrolysis. Crowded and smooth filamentous carbon materials with a similar morphology were observed in all the studied cases. No compelling evidence indicates a relationship between catalyst species and the morphology of formed carbon products. The high-magnification TEM images in Figure 6(b) and Figure S15 confirm the formation of highly ordered carbon nanotubes with outer diameters ranging from ~10-40 nm. The widely accepted formation mechanism for carbon nanotubes is the three-step "particle-wire-tube" process[28]: Carbon species are initially captured and transformed into nanoparticles, which subsequently self-assembled into nanowires. These nanowires further transform into nanotubes in the final step. As observed in the TEM-EDXS analysis in Figure 6(c) and Figure S15, Ni, Fe, and Co present in the studied SACs appear to serve as active sites for capturing carbon species and facilitating nanoparticle formation. It is important to note that when utilizing only CeO_2 support as a pre-catalyst, as depicted in Figure S16, no filamentous carbon materials were produced in the plasma-thermal catalytic process. The Temperature programmed Oxidation (TPO) analysis provided further confirmation of the carbon nanomaterial species. The derivative weight changes, as depicted in Figure S17 at around 530 °C for all studied cases can be linked to carbon nanotubes according to literature. The absence of obvious peaks at around 800 °C indicate that no carbon fibers have been generated in the process [27,29].

10.1002/anie.202404196

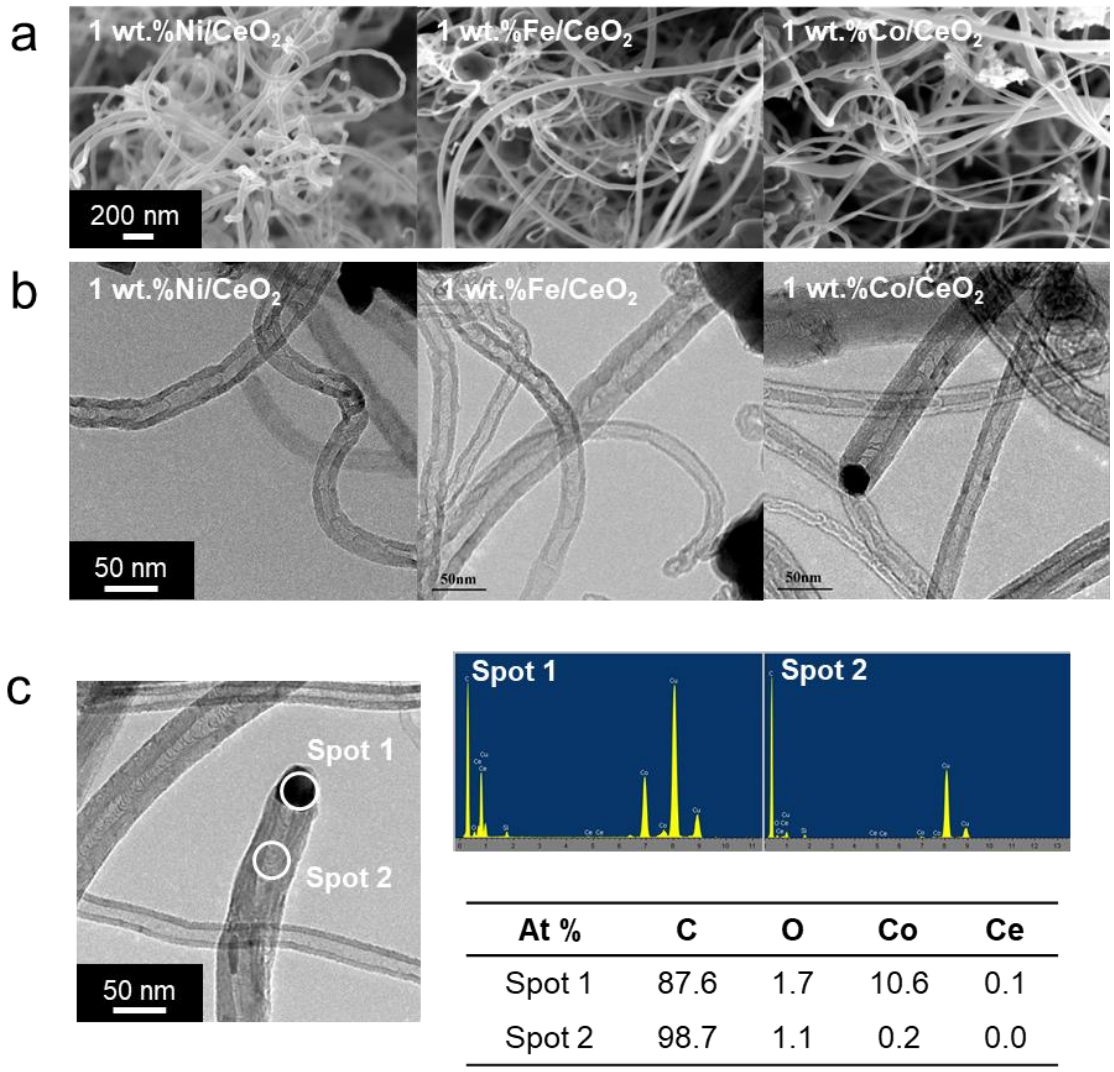

At %	C	O	Co	Ce
Spot 1	87.6	1.7	10.6	0.1
Spot 2	98.7	1.1	0.2	0.0

Figure 6. (a) SEM and (b) TEM images of the generated carbon nanomaterials via plasma-thermal catalytic pyrolysis over 1 wt.% *M*/CeO_2 (*M* = Ni, Co, Fe) single atom catalysts. (c) TEM with EDXS spectra of the produced carbon nanomaterials over1 wt.% Co/CeO_2. The element Cu is from the copper grid supporter.

The generated carbon materials were also analyzed with Raman spectroscopy to assess the purity and microstructural information of carbon nanotubes or nano filaments based on vibrational mode information (See Figure S18). The first sharp band appeared at 1350 cm^{-1} namely D band is due to the vibrational pattern with A_{1g} symmetry of amorphous or the disordered carbon[30]. G band comes at 1580 cm^{-1} referring to the vibrational mode with E_{2g} symmetry of arranged carbon atoms e.g., in graphite[31]. The intensity ratio of I_D/I_G is a quantitative index to evaluate the disorder degree and defect density. Low I_D/I_G ratios from all the studied cases indicate that the deposited carbon materials have a highly arranged

microstructure and limited defects. These results indicated that high quality carbon nanomaterials can be produced in the developed plasma-thermal catalytic pyrolysis approach. Apart from using single typed plastic, mixtures of multi-typed plastic wastes were also investigated, which succeed to generate high-quality CNTs as well (see Figure S19). Effective up-carbonatization of the carbon from real-world plastic wastes can be achieved via our innovated approach.

Proposed reaction scheme and comparison of energy yield of H_2 and performance with representative studies

Plasma-based methods are becoming increasingly popular for fuel and chemical synthesis due to the highly reactive nature of plasma, encompassing a range of reactive species such as electrons, various radicals, ions, excited species, and photons[32]. These reactive species are supposed to facilitate the cleavage of long chain polymers in a plasma pyrolysis of waste plastics. When initiating the plasma, plastics can immediately degrade into gases within seconds because of the high ionization of atoms coming from the collisions between polymers and reactive species of plasma. Subsequent collisions between the generated gas molecules and plasma included reactive species further breakdown the complex alkene and aromatic molecules into simple substances as shown in Figure 7(a). This proposed reaction mechanism is in great agreement with the findings from the results of catalyst-free plasma alone process, where H_2 and C_2H_2 are the two predominant products of the decomposition of different waste plastics (as shown in Figure 1(d) and Table S2). The highly energetic electron and excited species in plasma can effectively cleave chemical bonds in plastics, initiating the disintegration of larger C_xH_y molecules into smaller ones. A strong electric field further delivers energy to these reactive radicals, enhancing their reactivity in breaking C-H bonds and therefore narrow the product types. The unique nature of plasma differs it fundamentally from the traditional heating processes and microwave-initiated catalytic processes. Since both of them are relying on the mass transfer rate of molecular desorption. In summary, the proposed plasma methodology rapidly generates carbon nanomaterials and hydrogen, alongside the production of light alkenes and aromatics. These intermediates swiftly degrade to yield additional H_2 and carbon products. High H_2 yield and selectivity are achievable due to the significantly intensified energy density in the plasma volume, promoting exceptionally fast heating rates. Integrating the plasma pyrolysis with the thermal catalytic process can further boost H_2 yield and at the meanwhile reduce other chemical products towards high-purity H_2 and carbon nanomaterial productions.

In the plasma-thermal catalytic process, the catalyst is situated in a furnace positioned at a considerable distance from the plasma active zone. As a result, the reactive species generated by the plasma, such as H and e-, do not reach the catalyst's surface. Instead, these catalysts facilitate the dehydrogenation of C_xH_y gases produced by the plasma process, converting them into H_2 and carbon nanomaterials through a thermal catalytic process. To streamline the process and enhance our understanding of the specific pathways and catalytic mechanisms involved, density functional theory (DFT) calculations were performed. These calculations allowed us to compare simulation results with experimental observations. Detailed computational methods are provided in the supporting information. The energy of releasing a H-atom from C-H bonds in hydrocarbons to a free H atom is a key factor which can determine the gas yields and composition. Since ethylene (C_2H_4) and acetylene (C_2H_2) are the two primary by-products in the plasma-thermal catalytic pyrolysis process (as shown in Figure 1(d)), calculating the corresponding energy for each step of cleaving chemical bonds ($C_2H_4 \rightarrow C_2H_3 \rightarrow C_2H_2$ and $C_2H_2 \rightarrow C_2H \rightarrow C_2 \rightarrow 2C$) in these two hydrocarbons over the investigated catalysts were intended to get a better understanding of the enhanced H_2 production. The intermediates of C_2H_4 and C_2H_2 dissociation over the studied catalysts can be observed from Figure 7(b) and Figure S20. Based on the results displayed in Figure 7(c) and (d), the dissociation energy of the first H atom from a C-H bond in C_2H_4 is ranked as 1 wt.% Co/CeO_2 < 1 wt.% Ni/CeO_2 < 1 wt.% Fe/CeO_2, indicating that the first dehydrogenation step from C_2H_4 to C_2H_3+H over Co/CeO_2 catalyst was the most efficient comparing to the others. The process was exothermic and thermodynamic favorable with the Gibbs free energy change (ΔG) of –0.18 eV. The results of the calculations were consistent with the experimental observations, indicating that the utilization of the Co/CeO_2 catalyst resulted in the lowest selectivity towards C_2H_4. Following dehydrogenation, the resulting C_2H_3 species bind to the surface of the M atom, while the H atom forms H* (Figure 7(b)). Unlike the exothermic process of the first C-H bond dissociation, the subsequent dehydrogenation step from C_2H_3 to C_2H_2+H over Co/CeO_2 catalyst is endothermic, with a ΔG of +0.35 eV.

The initial H atom dissociation in other processes, such as $C_2H_2 \rightarrow C_2H \rightarrow C_2 \rightarrow 2C$, is also endothermic across all the catalysts studied, as indicated by the Gibbs energy values in Figure 7(d). Among these, Co/CeO_2 catalyst, with the lowest ΔG of +0.46 eV, is the most thermodynamically favorable. Similarly, the second H dissociation in the $C_2H \rightarrow C_2$+H process over Co/CeO_2 catalyst is more thermodynamically favorable compared to Fe/CeO_2 and Ni/CeO_2 catalysts, which require ΔG of +2.54 eV and +2.81 eV, respectively. Besides, the needed ΔG for the cleavage of the first C-H bond in C_2H_2 are higher than that in C_2H_4 over 1 wt.% Co/CeO_2

and 1 wt.% Ni/CeO_2 catalysts, illustrating that the dehydrogenation process of $C_2H_4 \rightarrow C_2H_3 \rightarrow C_2H_2$ is more attractive than the step from $C_2H_2 \rightarrow C_2H \rightarrow C_2 \rightarrow 2C$ from a thermodynamic aspect. It could be one of the reasons for the higher portion of C_2H_2 than C_2H_4 in the gaseous products observed from the experiments. Moreover, because of the discussed dissociation of C_2H_4 can also promote the formation of C_2H_2, which can be another reason for the higher C_2H_2 yield. DFT calculations further convinced that the designed 1 wt.% Co/CeO_2 single atom catalyst in this work is an active catalyst for plasma-enabled catalytic pyrolysis of waste plastics.

The H_2 yield in the developed plasma-enabled system can be further improved by optimizing the experimental system parameters, such as the N_2 flow rate of the plasma process, plasma power input, the distance between the plasma and plastic feedstock, and the reaction temperature for the catalysts. Additionally, modifying the size of the plastic waste feedstock may also enhance the H_2 yield. We conducted the catalyst-free plasma alone process and the plasma-thermal catalytic process using 1 wt.% Fe/CeO_2 under the same conditions with smaller-sized HDPE (~1 mm) instead of the larger size (~3 mm) used in this study. As shown in Figure S21, this adjustment significantly improved the H_2 yield and selectivity in the both processes. An impressive H_2 yield of 51.1 mmol/$g_{plastic}$ (equivalent to 71.6% of the theoretical H_2 production) with a selectivity of 75.7% can be achieved in the plasma-thermal catalytic process using the 1 wt.% Fe/CeO_2 catalyst. Future improvements in the efficiency of the catalysts, such as increasing the loading of active metal species in single-atom catalysts, are expected to further enhance the H_2 yield and selectivity of the developed process. The engineering of the plasma reactor is also expected to enhance the overall energy efficiency of the whole process.

Based on the results obtained in this work, the evolved H_2 yield and corresponding selectivity from waste plastics pyrolysis were compared with the data from recent literature (See Table S7). Our novel plasma-thermal catalytic process demonstrated an attractive performance both in the H_2 yield and H_2 selectivity, making it a promising upcycling method of plastic wastes via directly converting them to value-added products. The single atom catalysts with ultra-low metal loading of 1 wt.% employed in our approach showed its great advantage in the metal utilization rate, especially from economic aspect, comparing to the traditional supported metal catalysts. Furthermore, the developed catalyst-free plasma alone process can reach similar or even higher H_2 yield compared to two-stage thermal catalytic pyrolysis, illustrating this plasma pyrolysis process can be a considerable alternative method for plastic waste management. The energy yield of H_2 (g_{H2}/kWh) is a critical factor to evaluate the economic function of the designed process, which has not yet been discussed in the previous

studies. It illustrates directly the energy consumption for producing 1 g of H_2. The energy yield of H_2 (g_{H2}/kWh) is heavily influenced by the operating conditions, reactor size, feedstock type and the amount of feedstock used. Therefore, directly using literature data to calculate the energy yield of H_2 can be misleading. To mitigate the impact of differences in equipment parameters, operating conditions, and feedstock mass across various studies on the calculation of energy yield of H_2 (g_{H2}/kWh), we introduce several reasonable assumptions based on information from the literature to ensure a fair comparison. The detailed energy consumption calculation and the corresponding calculated energy yield of H_2 (g_{H2}/kWh) for different studies are concluded in the Table S7 and Figure 7(e) [14,15,18,20,21,23,26,27]. It can be observed clearly that the catalyst-free plasma alone process achieves higher energy yields of H_2 (g_{H2}/kWh) than most reported works due to the high efficiency of the plasma process with the short reaction time. It is more than 2 times higher than that of reported microwave-initiated catalytic process[20–23,26] and over 20 times higher than reported two-stage catalytic pyrolysis processes[14,15,27].

It is noteworthy that, although the plasma-thermal catalytic process shows less attractive energy yield results for H_2 when compared to a single batch feedstock, considering a continuous process as depicted in in Table S8 and Figure 7(f), the energy yield of H_2 (g_{H2}/kWh) significantly increases with longer reaction times. Integrating the plasma process with a thermal catalytic process as a tandem technology not only enhances hydrogen production but also yields carbon nanotubes. Importantly, a range of potential catalytic materials can be employed. Since the plastic and catalyst are separate, allowing for the consistent transformation of diverse types of plastic waste streams into valuable products, which also provide a promising way for avoiding catalyst deactivation. In contrast, the microwave-initiated catalytic process requires absorptive materials with catalytic functions to absorb microwave energy. For plastic decomposition to occur in this procedure, the catalyst must be uniformly mixed with the plastic. These stringent requirements pose considerable challenges for achieving consistent transformation of plastic waste streams in the microwave-initiated catalytic process. Considering scaling up the developed plasma-enabled approach process to a larger scale with continuous feedstock feeding in the future, the heat generated from plasma pyrolysis can be directly utilized for activating the catalysts in the tandem second stage, which could further improve the overall energy efficiency of the whole process.

10.1002/anie.202404196

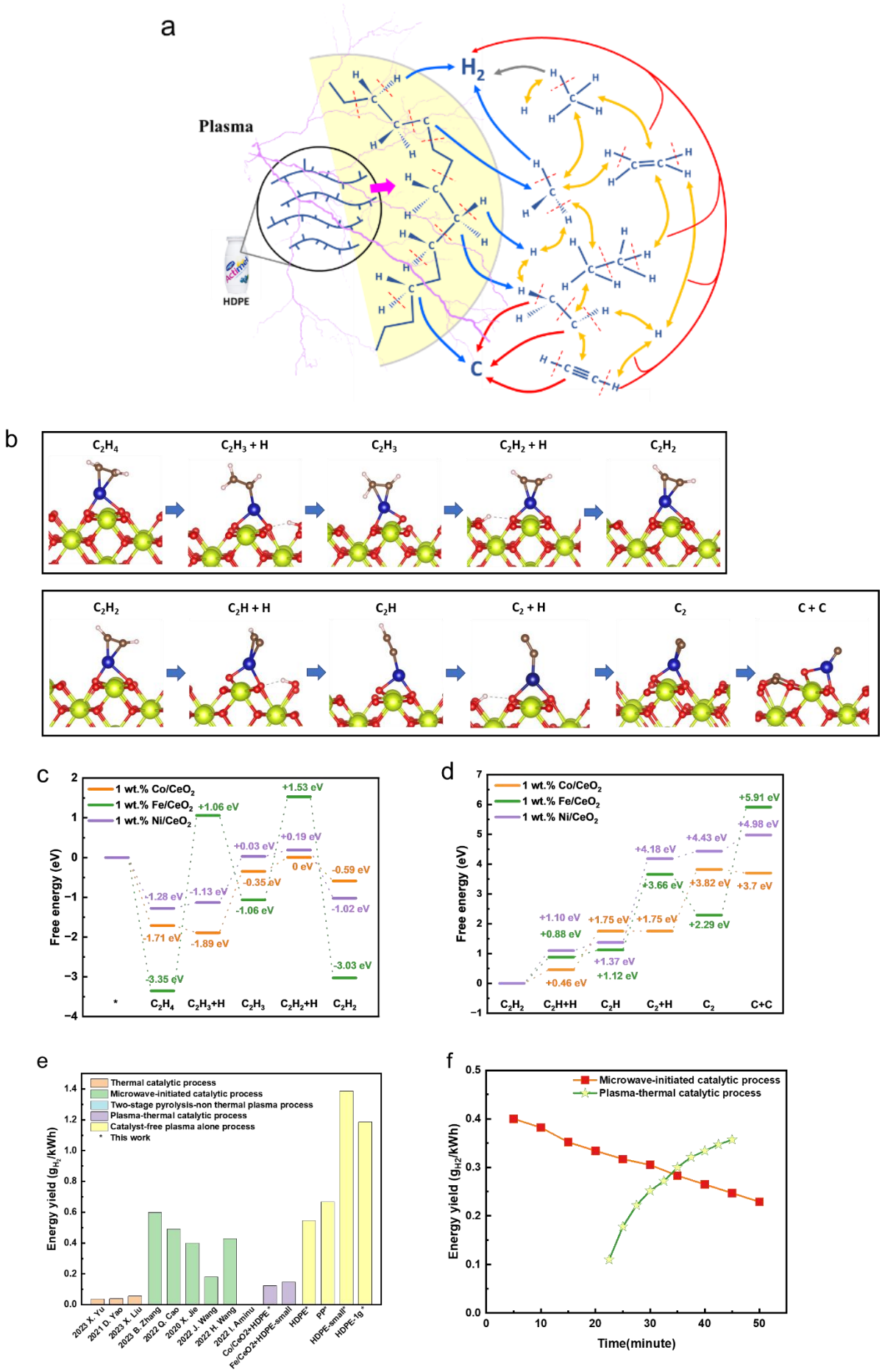

Figure 7. (a) Schematic of the possible reaction scheme of the plasma alone pyrolysis of discarded milk containers (HDPE) (b) Transition state geometries of C_2H_4 and C_2H_2 dehydrogenation over 1 wt.% Co/CeO_2 single atom catalyst. (c) Gibbs free energy from DFT calculation in cases of C_2H_4 and C_2H_2 dehydrogenation over 1 wt.% *M*/CeO_2 (M = Ni, Co, Fe) single atom catalysts. (d) Energy yield (g_{H2}/kWh) comparison of recent studies for H_2 production from waste plastics. (e) Energy yield (gH_2/kWh) of state-of-the-art processes for H_2 production from plastic wastes. (f) Energy yield (g_{H2}/kWh) comparison of the cycle tests between the reported microwave-initiated catalytic process[20] and the plasma-thermal catalytic pyrolysis process in this work.

Conclusions

In this work, we reported a novel plasma-enabled approach for effective upcycling of single and multi-typed plastic wastes collected from daily life into H_2-rich gases and value-added carbon products. The one-step catalyst-free plasma alone process is very promising for waste plastic management as it shows a great potential in the recycling of mixed plastic wastes within a very short reaction time, which can directly convert the waste mixtures into H_2-rich gases without extra sorting process or pretreatment. When coupling the thermal catalytic process into the plasma pyrolysis process, a significant increase in both H_2 production and selectivity can be identified. Notably, that the H_2 yields obtained with a 1 wt.% Fe/CeO_2 single-atom catalyst and a 10 wt.% Fe/CeO_2 nanoparticle catalyst are comparable. This finding shown by using the single atom catalysts provides a viable route for the economical and productive recycling of plastic wastes. It is also important to observe that the developed plasma-thermal catalytic approach can effectively break down the multi-typed plastic waste mixtures with ~100% of hydrogen atom recovery efficiency, leading to the efficient H_2 production. The spent catalysts after five successive cycles were also characterized by XRD (Rietveld refinements), STEM and XAS techniques and the results demonstrated that the studied catalysts are still generally maintaining the same coordination/structure. A high hydrogen yield of 42.9 mmol / $g_{plastic}$ was maintained even after 10 cycles of successive measurements and the highest H_2 yield of 46.7 mmol / $g_{plastic}$ (equivalent to 64.4% of theoretical H_2 production) was achieved at the 7th cycle, which demonstrates an excellent ability of transformation of plastics to H_2 and high value carbon products in coupling plasma pyrolysis process with thermal catalytic process. By combining experimental and computational approaches, we have gained a better understanding of the possible catalytic dehydrogenation mechanisms employed by the investigated single-atom catalysts in the developed plasma-enabled process. The developed plasma-enabled

approach offers an appealing solution to the pressing issue of plastic waste accumulation, which has serious environmental effects and creates difficulties for waste management. The presented approach can be a cost-effective, productive, and selective way of directly transforming complex plastic wastes into valuable products.

Acknowledgments

The authors are thankful to Maria Kunkel, Regine Peter, and Thomas Windhagen for their kind support during the gas product and plastic analysis, BET measurements, and preparations of the catalytic experiments. We thank the help of Dr. Kaiwen Wang for conducting STEM. We thank the staff at the BL11B beamline of the Shanghai Synchrotron Radiation Facility for assistance with the XAFS. G.C., G.H., and A.W. kindly thank the Hydrogen performance center in Hesse for financial support during the Green materials for Green H_2 project. Y.Z and Z.H thank the Natural Science Foundation of China (52325401 and 202209136) for financial support. Z.R. thanks the China Postdoctoral Foundation (GYB20230013) for financial support.

Conflict of interest

The authors declare no conflict of interest.

References

[1] Plastics Europe, "Plastics – the fast Facts 2023 • Plastics Europe", can be found under https://plasticseurope.org/knowledge-hub/plastics-the-fast-facts-2023/, **2023**.

[2] a) *The circular economy—a powerful force for climate mitigation*, **2018**; b) H. Sardon, A. P. Dove, *Science (New York, N.Y.)* **2018**, *360*, 380.

[3] I. S. Lase, D. Tonini, D. Caro, P. F. Albizzati, J. Cristóbal, M. Roosen, M. Kusenberg, K. Ragaert, K. M. van Geem, J. Dewulf et al., *Resources, Conservation and Recycling* **2023**, *192*, 106916.

[4] F. Ramzan, B. Shoukat, M. Y. Naz, S. Shukrullah, F. Ahmad, I. Naz, M. M. Makhlouf, M. U. Farooq, K. Kamran, *Thermochimica Acta* **2022**, *715*, 179294.

[5] *Global plastics outlook. Policy scenarios to 2060 / [OECD]*, OECD Publishing, [Paris], **2022**.

[6] Plastics Europe, "Plastics - the Facts 2022 • Plastics Europe", can be found under https://plasticseurope.org/knowledge-hub/plastics-the-facts-2022-2/, **2023**.

[7] J. Choi, I. Yang, S.-S. Kim, S. Y. Cho, S. Lee, *Macromolecular rapid communications* **2022**, *43*, e2100467.

[8] a) I. Vollmer, M. J. F. Jenks, M. C. P. Roelands, R. J. White, T. van Harmelen, P. de Wild, G. P. van der Laan, F. Meirer, J. T. F. Keurentjes, B. M. Weckhuysen, *Angewandte Chemie International Edition* **2020**, *59*, 15402; b) I. Vollmer, M. J. F. Jenks, R. Mayorga González, F. Meirer, B. M. Weckhuysen, *Angewandte Chemie International Edition* **2021**, *60*, 16101.

[9] a) Subhashini, T. Mondal, *Journal of Environmental Management* **2023**, *344*, 118680; b) M. F. Paucar-Sánchez, M. A. Martín-Lara, M. Calero, G. Blázquez, R. R. Solís, M. J. Muñoz-Batista, *Fuel* **2023**, *352*, 129145.

[10] R. A. Muñoz Meneses, G. Cabrera-Papamija, F. Machuca-Martínez, L. A. Rodríguez, J. E. Diosa, E. Mosquera-Vargas, *Heliyon* **2022**, *8*, e09028.

[11] a) Le Zhang, D. Yao, T.-H. Tsui, K.-C. Loh, C.-H. Wang, Y. Dai, Y. W. Tong, *Journal of Environmental Management* **2022**, *306*, 114471; b) F. Manenti, A. Galeazzi, F. Negri, K. Prifti in *Advances in synthesis gas. Methods, technologies and applications* (Eds.: M. R. Rahimpour, M. A. Makarem, M. Meshksar), Elsevier, Amsterdam, Netherlands, Oxford, United Kingdom, Cambridge, MA, **2023-**, pp. 457–474.

[12] G. Chen, X. Tu, G. Homm, A. Weidenkaff, *Nat Rev Mater* **2022**, *7*, 333.

[13] K. A. Graves, L. J. Higgins, M. A. Nahil, B. Mishra, P. T. Williams, *Journal of Analytical and Applied Pyrolysis* **2022**, *161*, 105396.

[14] X. Liu, D. Xu, H. Ding, M. Widenmeyer, W. Xie, M. Mellin, F. Qu, G. Chen, Y. S. Zhang, Z. Zhang et al., *Applied Catalysis B: Environmental* **2023**, *324*, 122271.

[15] D. Yao, H. Li, Y. Dai, C.-H. Wang, *Chemical Engineering Journal* **2021**, *408*, 127268.

[16] a) P. T. Williams, *Waste Biomass Valor* **2021**, *12*, 1; b) Y. Peng, Y. Wang, L. Ke, L. Dai, Q. Wu, K. Cobb, Y. Zeng, R. Zou, Y. Liu, R. Ruan, *Energy Conversion and Management* **2022**, *254*, 115243; c) M. Jiang, X. Wang, W. Xi, H. Zhou, P. Yang, J. Yao, X. Jiang, D. Wu, *Chemical Engineering Journal* **2023**, *461*, 141962; d) D. Xu, C. Shen, X. Liu, W. Xie, H. Ding, M. Widenmeyer, M. Mellin, F. Qu, A. Rashid, G. Chen et al., *Chemical Engineering Journal* **2023**, *476*, 146477.

[17] a) I. Aminu, M. A. Nahil, P. T. Williams, *Energy Fuels* **2020**, *34*, 11679; b) I. Aminu, M. A. Nahil, P. T. Williams, *Catalysis Today* **2023**, *420*, 114084.

[18] I. Aminu, M. A. Nahil, P. T. Williams, *Energy Fuels* **2022**, *36*, 3788.

[19] W. Li, K. Qian, Z. Yang, X. Ding, W. Tian, D. Chen, *Applied Catalysis B: Environmental* **2023**, *327*, 122451.

[20] X. Jie, W. Li, D. Slocombe, Y. Gao, I. Banerjee, S. Gonzalez-Cortes, B. Yao, H. AlMegren, S. Alshihri, J. Dilworth et al., *Nat Catal* **2020**, *3*, 902.

[21] H. Wang, B. Zhang, P. Luo, K. Huang, Y. Zhou, *Processes* **2022**, *10*, 782.

[22] J. Wang, Y. Pan, J. Song, Q. Huang, *Journal of Analytical and Applied Pyrolysis* **2022**, *166*, 105612.

[23] B. Zhang, H. Wang, Y. Yang, Y. Zhou, B. Zhang, K. Huang, *Journal of Environmental Chemical Engineering* **2023**, *11*, 109710.

[24] J. Ge, D. Zhang, Y. Qin, T. Dou, M. Jiang, F. Zhang, X. Lei, *Applied Catalysis B: Environmental* **2021**, *298*, 120557.

[25] a) M. Muhyuddin, P. Mustarelli, C. Santoro, *ChemSusChem* **2021**, *14*, 3785; b) J. C. Park, J.-C. Kim, S. Park, D.-W. Kim, *Applied Surface Science* **2020**, *510*, 145505; c) A. Veksha, K. Yin, J. G. S. Moo, W.-D. Oh, A. Ahamed, W. Q. Chen, P. Weerachanchai, A. Giannis, G. Lisak, *Journal of Hazardous Materials* **2020**, *387*, 121256.

[26] Q. Cao, H.-C. Dai, J.-H. He, C.-L. Wang, C. Zhou, X.-F. Cheng, J.-M. Lu, *Applied Catalysis B: Environmental* **2022**, *318*, 121828.

[27] X. Yu, G. Chen, M. Widenmeyer, I. Kinski, X. Liu, U. Kunz, D. Schüpfer, L. Molina-Luna, X. Tu, G. Homm et al., *Applied Catalysis B: Environmental* **2023**, *334*, 122838.

[28] G. Du, S. Feng, J. Zhao, C. Song, S. Bai, Z. Zhu, *Journal of the American Chemical Society* **2006**, *128*, 15405.

[29] G. Chen, X. Yu, K. Ostrikov, B. Liu, J. Harding, G. Homm, H. Guo, S. Andreas Schunk, Y. Zhou, X. Tu et al., *Chemical Engineering Journal* **2023**, *476*, 146335.

[30] a) S. D. M. Brown, A. Jorio, M. S. Dresselhaus, G. Dresselhaus, *Phys. Rev. B* **2001**, *64*; b) A. C. Ferrari, J. Robertson, *Phys. Rev. B* **2000**, *61*, 14095.

[31] a) S. D. M. Brown, A. Jorio, P. Corio, M. S. Dresselhaus, G. Dresselhaus, R. Saito, K. Kneipp, *Phys. Rev. B* **2001**, *63*; b) L. M. Malard, M. A. Pimenta, G. Dresselhaus, M. S. Dresselhaus, *Physics Reports* **2009**, *473*, 51.

[32] a) W. Bongers, H. Bouwmeester, B. Wolf, F. Peeters, S. Welzel, D. van den Bekerom, N. den Harder, A. Goede, M. Graswinckel, P. W. Groen et al., *Plasma Processes & Polymers* **2017**, *14*; b) L. Hollevoet, F. Jardali, Y. Gorbanev, J. Creel, A. Bogaerts, J. A. Martens, *Angewandte Chemie* **2020**, *132*, 24033; c) G. Chen, R. Snyders, N. Britun, *Journal of CO2 Utilization* **2021**, *49*, 101557; d) Y. Wang, W. Yang, S. Xu, S. Zhao, G. Chen, A. Weidenkaff, C. Hardacre, X. Fan, J. Huang, X. Tu, *Journal of the American Chemical Society* **2022**, *144*, 12020; e) H. Liang, F. Ming, H. N. Alshareef, *Advanced Energy Materials* **2018**, *8*.